UC San Diego
UC San Diego Previously Published Works

Title
Conserved Noncoding Elements in the Most Distant Genera of Cephalochordates: The Goldilocks Principle

Permalink
https://escholarship.org/uc/item/6s59h2w6

Journal
Genome Biology and Evolution, 8(8)

ISSN
1759-6653

Authors
Yue, Jia-Xing
Kozmikova, Iryna
Ono, Hiroki
et al.

Publication Date
2016-08-01

DOI
10.1093/gbe/evw158

Peer reviewed

eScholarship.org Powered by the California Digital Library
University of California

Conserved Noncoding Elements in the Most Distant Genera of Cephalochordates: The Goldilocks Principle

Jia-Xing Yue,[1,5] Iryna Kozmikova,[2] Hiroki Ono,[3] Carlos W. Nossa,[1,6] Zbynek Kozmik,[2] Nicholas H. Putnam,[1,7] Jr-Kai Yu,[4] and Linda Z. Holland[3,*]

[1]Biosciences at Rice, Rice University, Houston, Texas

[2]Department of Transcriptional Regulation, Institute of Molecular Genetics, Prague 14220, Czech Republic

[3]Marine Biology Research Division, Scripps Institution of Oceanography, UC San Diego, La Jolla, California

[4]Institute of Cellular and Organismic Biology, Academia Sinica, Taipei, Taiwan

[5]Present address: Institute for Research on Cancer and Aging, Nice (IRCAN), CNRS UMR 7284, INSERM U1081, Nice 06107 France

[6]Present address: Gene by Gene Ltd., Houston, TX 77008

[7]Present address: Dovetail Genomics, Santa Cruz, CA 95060

*Corresponding author: E-mail: lzholland@ucsd.edu.

Accepted: June 22, 2016

Data deposition: This project has ben deposited at the Sequence Read Archive (SRA) under the accession number PRJA280114.

Abstract

Cephalochordates, the sister group of vertebrates + tunicates, are evolving particularly slowly. Therefore, genome comparisons between two congeners of *Branchiostoma* revealed so many conserved noncoding elements (CNEs), that it was not clear how many are functional regulatory elements. To more effectively identify CNEs with potential regulatory functions, we compared noncoding sequences of genomes of the most phylogenetically distant cephalochordate genera, *Asymmetron* and *Branchiostoma*, which diverged approximately 120–160 million years ago. We found 113,070 noncoding elements conserved between the two species, amounting to 3.3% of the genome. The genomic distribution, target gene ontology, and enriched motifs of these CNEs all suggest that many of them are probably *cis*-regulatory elements. More than 90% of previously verified amphioxus regulatory elements were re-captured in this study. A search of the cephalochordate CNEs around 50 developmental genes in several vertebrate genomes revealed eight CNEs conserved between cephalochordates and vertebrates, indicating sequence conservation over > 500 million years of divergence. The function of five CNEs was tested in reporter assays in zebrafish, and one was also tested in amphioxus. All five CNEs proved to be tissue-specific enhancers. Taken together, these findings indicate that even though *Branchiostoma* and *Asymmetron* are distantly related, as they are evolving slowly, comparisons between them are likely optimal for identifying most of their tissue-specific *cis*-regulatory elements laying the foundation for functional characterizations and a better understanding of the evolution of developmental regulation in cephalochordates.

Key words: CNE, regulatory element, cephalochordate, asymmetron, amphioxus.

Introduction

Noncoding DNA includes several classes of functional elements that are phylogenetically conserved. Some of the best-known are microRNAs (miRNAs) (Hausser and Zavolan 2014) and their target sequences, long noncoding RNAs of several types (Fatica and Bozzoni 2014), and gene regulatory sequences (Guil and Esteller 2012; Nelson and Wardle 2013; Fatica and Bozzoni 2014). Many of these noncoding elements have characteristic sequences that can be used to identify them, but *cis*-regulatory regions of genes, which consist of constellations of transcription factor binding sites, are less stereotyped. As they typically reside either in regions flanking coding sequences or within introns, the initial strategy to identify them was to clone introns or a few thousand base pairs of flanking sequences into a reporter plasmid and determine if the potential regulatory DNA directs tissue-specific expression in embryos. Once this relatively large piece is determined to contain a transcriptional enhancer, it can be pared down to

© The Author 2016. Published by Oxford University Press on behalf of the Society for Molecular Biology and Evolution.
This is an Open Access article distributed under the terms of the Creative Commons Attribution Non-Commercial License (http://creativecommons.org/licenses/by-nc/4.0/), which permits non-commercial re-use, distribution, and reproduction in any medium, provided the original work is properly cited. For commercial re-use, please contact journals.permissions@oup.com

determine the precise sequences that constitute the enhancer. This traditional strategy works well but is cumbersome.

Recently, high-throughput approaches based on assessing chromatin state (methylation and acetylation) (e.g. ChIP-seq) and accessibility (e.g. DNaseI-seq, ATAC-seq) were applied to identify potential regulatory elements in the whole genome of a single species (Valouev et al. 2008; Buenrostro et al. 2013; Stergachis et al. 2014; Martinez-Morales 2015). However, such high-throughput approaches without concomitant analysis of transcription factor binding can lead to high false positives (Dogan et al. 2015). Neither of these methods directly addresses the question of how enhancers have changed during evolution of new traits and new species.

For understanding the evolution of regulatory DNA, comparative genomics has been useful. As more and more genomes became available, computational comparisons of genomes that are neither too closely nor too distantly related have identified large numbers of potential regulatory sequences, typically a few hundred base pairs long. These conserved noncoding elements (CNEs) can be experimentally tested for regulatory activity by linking them to a reporter gene such as green fluorescent protein (*GFP*) or *LacZ* and introducing them into eggs or embryos. This combined approach of *in silico* sequence conservation profiling, followed by elimination of sequences matching miRNAs and other known elements, followed by *in vivo* testing of the remaining sequences for gene regulatory activity has been successful in identifying many functional *cis*-regulatory elements (Woolfe et al. 2005; Pennacchio et al. 2006; McEwen et al. 2009; Hemberg et al. 2012). Moreover, comparisons of these elements across larger phylogenetic distances can reveal their origin and evolutionary fates along different lineages (Lang et al. 2010; Braasch et al. 2016). In general, many CNEs seem to be lineage-specific with high turnover rate even between closely-related species (Meader et al. 2010; Hiller et al. 2012), but some CNEs have been found to be extremely evolutionarily conserved even across different phyla (Royo et al. 2011; Clarke et al. 2012). The evolution of *cis*-regulatory elements has been considered to be the all-important factor in creating phenotypic diversity (Davidson 2011), and while it has more recently been shown that evolution of proteins is also highly important (Ono et al. 2014), the evolution of *cis*-regulation remains key to understanding phenotypic diversity.

One important consideration of studying CNEs via comparative genomics is that if the genome sequences of the organisms being compared are too much alike, the background noise will be too high for the CNEs to stand out. Conversely, when the genome sequences are too different, there may be no conservation outside of coding regions. This is the Goldilocks principle. The genome sequences of the organisms being compared must differ just the right amount from one another—not too little or too much. Thus, for vertebrates, whose genomes are evolving moderately slowly, comparisons between human and a teleost fish revealed 1,400 CNEs, 90% of which were functional (Woolfe et al. 2005), while comparisons among somewhat more closely related vertebrates yielded up to 3,000 CNEs, many of which were verified as functional regulatory elements (Ishibashi et al. 2012; Parker et al. 2014; Martinez-Morales 2015; Yousaf et al. 2015). In contrast, relatively few CNEs were shown by comparisons of the genomes of fast-evolving tunicates and vertebrates and many of those were not in syntenic loci (Maeso et al. 2013; Sanges et al. 2013). It took comparisons between two species within the same genus that separated only 3 million years ago (mya) to reveal additional CNEs in tunicates (Doglio et al. 2013). For cephalochordates, which are evolving exceptionally slowly (Yue et al. 2014), comparisons with fish and mouse identified about 670 such CNEs but only half of 42 tested for regulatory activity drove expression in zebrafish embryos (Hufton et al. 2009). However, with >20,000 genes in a cephalochordate genome (Putnam et al. 2008), there must be many thousands more CNEs. The phylogenetic distance between cephalochordates and vertebrates is evidently too great for most regulatory elements to be readily identified. This is exemplified by comparison of the *Hedgehog* locus between *Branchiostoma* and vertebrates, which showed there was virtually no conservation of noncoding DNA sequences. In contrast, comparisons of the *Hedgehog* locus among three species of *Branchiostoma* (*Branchiostoma lanceolatum*, *Branchiostoma floridae*, and *Branchiostoma belcheri*) revealed altogether too much conservation of noncoding DNA sequences for regulatory elements to be readily identified (Pascual-Anaya et al. 2008; Irimia et al. 2012a). Moreover, comparison of whole genome sequences of *B. belcheri* and *B. floridae*, which diverged about 112 mya (Nohara et al. 2005), revealed up to 180,000 CNEs (Huang et al. 2014). Many of these are likely due to insufficient divergence rather than functional constraints. Thus, the genomic sequences of *Branchiostoma* species are too close while those of *Branchiostoma* and vertebrates are too different for ready identification of CNEs and understanding their evolution. Therefore, we compared genomes of *Asymmetron lucayanum* and *B. floridae*, which diverged about 120–160 mya. We found that these genomes differ just about the right amount with approximately 113,000 CNEs. Some of these may not be functional regulatory elements. If they were, that would mean about five regulatory elements per gene, which is not altogether unreasonable, as some might be enhancers and others repressors. Even so, included in this set of CNEs were most of those previously identified as being conserved with vertebrates. We performed functional tests for five amphioxus CNEs that are not conserved with vertebrates at the sequence level and confirmed that they are indeed regulatory elements. Interestingly, when expressed in zebrafish, one of these CNEs directed expression to a domain that normally does not express the gene. Therefore, while the function of CNEs may be conserved across wide evolutionary distances, the genes they regulate may not always be conserved.

Materials and Methods

Whole Genome Shotgun Sequencing

We used three adult animals (two males and one female) and 22 larvae (from the cross of two of those three adults) for this study. The adult animals were collected from Bimini, Bahamas and maintained in the laboratory. The DNA of one male was used to make the first two libraries—one short-insert (approximately 300 bp) library and one long-insert (approximately 5,000 bp) library. We denoted these two libraries as Aluca4 and Aluca15, respectively. A moonlight regime (Fishbowl Innovations, Spokane, WA) was used to induce the spawning of another male and a female. The DNA of this pair with 22 of their offspring was used to make an additional pooled library (approximately 300 bp insert size and individually barcoded). We denoted this library as Aluca39. The genomic DNA of all samples was extracted by the DNAEasy kit (Qiagen Inc., Valencia CA, USA) and sequencing libraries were prepared by the Nextera kit (Illumina Inc, San Diego, CA, USA), according to the manufacturers' protocols. Illumina paired-end sequencing was performed in three separate lanes on the Illumina HiSeq2000 platform. Aluca4 was sequenced at the Human and Molecular Genetics Center, Medical College of Wisconsin (Milwaukee, WI, USA). Auca15 and Aluca39 were sequenced at BGI (Shenzhen, Guangdong, China). The raw sequencing data are available from the NCBI SRA database via NCBI BioProject accession PRJNA280114 and PRJNA301923.

Whole-Genome Shotgun Sequencing Reads Processing and *k*-Mer Analysis

For each whole genome sequencing (WGS) library, raw reads were trimmed by Trimmomatic (v0.32) (Bolger et al. 2014) and processed by Deconseq (v0.4.3) (Schmieder and Edwards 2011a) to remove potential contaminations. For *k*-mer analysis, the reads from Aluca4 were counted by Jellyfish (v2.0) (Marçais and Kingsford 2011) using the two-pass method described in its manual. Different values of *k* (17, 19, 21, 23, and 25) were explored independently. The multiplicity of each *k*-mer and the number of distinct *k*-mers given such multiplicity were summarized.

Whole Genome Shotgun Sequencing Data Assembly

We used Platanus (v1.2.1) (Kajitani et al. 2014) to generate a *de novo* assembly for *A. lucayanum* with trimmed WGS reads from the Aluca4 and Aluca15 libraries, which were from the same animal. We chose Platanus because it was designed to handle highly heterozygous genomes. The maximum difference for bubble crush (-u) was set as 0.2 following the suggestion of the Platanus user manual for highly heterozygous genomes. The statistical summary for the assembly result was calculated by NGSQCToolkit (v2.3) (Patel and Jain 2012). This genome assembly has been deposited at DDBJ/ENA/GenBank under the accession LZCU00000000. The version described in this article is the version LZCU01000000.

Whole Genome Shotgun Reads Mapping

For each animal sample, the software package Stampy (v1.0.23) (Lunter and Goodson 2011) with "divergence" set to 10% was used to map trimmed reads to the *B. floridae* reference genome (v2.0) (Putnam et al. 2008). The mapping alignments were further processed with three programs 1) SAMtools (v0.1.19) (Li et al. 2009), 2) Picard-Tools (v1.106) (http://broadinstitute.github.io/picard/, last accessed July 20, 2016), and 3) GATK (v2.8-1) (McKenna et al. 2010). Depth of coverage across the reference genome was calculated by GATK with a mapping quality cutoff of 20.

RNA-Seq Sequencing and Assembly

The sequencing data from four RNA-Seq libraries used for this study included the following: 1) pooled *A. lucayanum* adults (denoted as asymAD), 2) pooled *A. lucayanum* 20h-larvae (phylotypic stage) (denoted as asym20h), 3) pooled *B. floridae* 20h-larvae (phylotypic stage) (denoted as bf20h), and 4) pooled *B. floridae* adults (denoted as bfAD). Details of reads processing and transcriptome assembly of the two *A. lucayanum* RNA-Seq libraries were previously described (Yue et al. 2014). The raw reads of these two *A. lucayanum* RNA-Seq libraries have been deposited in NCBI SRA database via NCBI BioProject accession PRJNA235900. The raw asymAD transcriptome assembly has been deposited at DDBJ/EMBL/GenBank under the accession GESY00000000 and version number GESY01000000. The raw asym20h transcriptome assembly has been deposited at DDBJ/EMBL/GenBank under the accession GETC00000000 and version number GETC01000000. The *B. floridae* pooled 20h-larvae library was prepared by the RNA-Seq kit (NuGen Inc., San Carlos, CA, USA) and sequenced by the Illumina GAII platform (paired-end 100 bp at the BioGem facility at University of California, San Diego, La Jolla, CA, USA). About 204 million raw reads were obtained for the bf20h library. Raw sequences are in the NCBI SRA database via NCBI BioProject accession PRJNA280115. The *B. floridae* pooled adults RNA-Seq library was constructed by as described by Fidler et al. (2014). The raw reads were deposited in NCBI SRA database (accession number: PRJNA215261). We processed the bf20h and bfAD RNA-Seq data following the same protocol as for the two *Asymmetron* libraries: raw reads were processed by Trimmomatic (v0.32) (Bolger et al. 2014), prinseq (v0.20.4) (Schmieder and Edwards 2011b), and Deconseq (v0.4.3) (Schmieder and Edwards 2011a) sequentially to trim the sequence and remove potential contamination; Trinity (r20131110) (Grabherr et al. 2011) and TransDecoder (http://transdecoder.github.io/, last accessed July 20, 2016) were used to generate the transcriptome assembly and infer the likely coding sequences (CDSs). The raw bf20h

transcriptome assembly has been deposited at DDBJ/EMBL/GenBank under the accession GESZ00000000 and version number GESZ01000000. The raw bfAD transcriptome assembly has been deposited at DDBJ/EMBL/GenBank under the accession GETA00000000 and version number GETA01000000.

Genome Size Estimation

We used the *k*-mer-based method to estimate the genome size of *A. lucayanum*. The *k*-mer multiplicity distribution curve contains three peaks: the error peak with multiplicity (0-3), the heterozygous peak with multiplicity of $d_k/2$, and the homozygous peak with multiplicity of d_k, where d_k is the *k*-mer depth of coverage. We used the 21-mer-multiplicity distribution to estimate the genome size. Assuming that N_k is the total number of non-error *k*-mers (after excluding the error peak from the *k*-mer multiplicity distribution), then the genome size G can be estimated by N_k/d_k.

Repeat and Coding Sequence Masking for the *B. floridae* Reference Genome

To facilitate CNE identification, we created a copy of a repeat-and-coding-masked *B. floridae* genome as follows: we first performed repeat-masking for the reference genome using the software package RepeatMasker (open-v4.0.3) (http://www.repeatmasker.org, last accessed July 20, 2016) together with the *B. floridae*'s repeats library (retrieved from http://genome.jgi.doe.gov/Brafl1/Brafl1.home.html, last accessed July 20, 2016). Then we masked all the *B. floridae* CDS regions based on a previously corrected copy of *B. floridae* gene annotation file (Yue et al. 2014). To exclude potential CDS regions as cleanly as possible, we used Exonerate (v2.2.0) (Slater and Birney 2005) to align the inferred CDSs from our *A. lucayanum* and *B. floridae* RNA-Seq assemblies to the *B. floridae* reference and further masked those matched regions. After masking, the remaining unmasked regions along the *B. floridae* reference assembly should represent the noncoding and non-repetitive portion of the *B. floridae* genome.

Identification of CNEs Shared between *Asymmetron* and *Branchiostoma* and between Two *Branchiostoma* Species

Two methods were adopted to identify CNEs shared between *Asymmetron* and *Branchiostoma*. The first is a whole-genome-alignment-based (WGA-based) method. In this method, we used the progressive Cactus pipeline (Paten et al. 2011) to align our fragmented genome assembly of *A. lucayanum* to the *B. floridae* v2.0 reference assembly. To identify highly conserved regions shared between these two species, the *Asymmetron-Branchiostoma* whole genome alignments were analyzed by VISTA (v1.4.26) (Frazer et al. 2004) with *B. floridae* as the reference and the criteria of 45-bp sliding window, 90% identity, and 45-bp minimal length. The intersection of the highly conserved regions identified by VISTA and the repeat-and-coding-masked *B. floridae* reference genome formed our preliminary set of WGA-based CNEs. The second method is cross-species-reads-mapping-based (CSRM-based). In this method, we took the *A. lucayanum*-to-*B. floridae* reads mapping alignment and masked all the regions covered by < 5 reads (mapping quality cutoff = 20) along the *B. floridae* reference genome. To form our preliminary set of CSRM-based CNEs, the unmasked regions after such mapping-depth masking were used to identify the intersections with the repeat-and-coding-masked *B. floridae* reference genome.

We annotated the noncoding RNAs (ncRNAs) contained in our preliminary CNE sets with a combination of BLASTN and an Infernal (v1.0.2) (Nawrocki et al. 2009) search using the wrapper script rfam_scan.pl provided by Rfam, against the Rfam database (v11.0) (Gardner et al. 2011). The miRNAs were further annotated by miRBase (Release 21) (Kozomara and Griffiths-Jones 2013). To further exclude potential coding sequences in our preliminary CNE sets, we trained AUGUSTUS (v3.0.2) (Stanke et al. 2004) with the gene annotation information for the *B. floridae* reference genome and subsequently performed *ab initio* gene prediction for our preliminary CNE sets. This identified likely CDS sequences that were not previously identified based on the reference *B. floridae* gene annotation and our four RNA-Seq libraries. After eliminating all annotated ncRNAs and likely CDS regions, we applied a final length cutoff of 45 bp for the remaining CNEs to form the final version of the cephalochordate CNE sets for the WGA-based method and CSRM-based method. Bedtools (v2.22.0) (Quinlan and Hall 2010) was used to take the intersection and union of these two final CNE sets to form another two CNE sets: the CNEs-intersection and CNEs-union sets. Neighboring CNEs that are <10 bp away were rejoined together as a single CNE. The raw sequences of WGA-based CNEs for *A. lucayanum–B. floridae* comparison were deposited at GitHub (https://github.com/yjx1217/SupplementaryData_for_Asymmetron_CNE_paper_2016.git, last accessed July 20, 2016).

In parallel, we also identified WGA-based CNEs based on the comparison between two *Branchiostoma* species (*B. floridae* and *B. belcheri*) for downstream analysis. The genome assembly and gene annotation information of *B. belcheri* used for this analysis were retrieved from http://mosas.sysu.edu.cn/genome/download_data.php, last accessed July 20, 2016 (v18h27.r3) (Huang et al. 2014). The raw sequences of WGA-based CNEs for *B. floridae–B. belcheri* comparison were also deposited at GitHub (https://github.com/yjx1217/SupplementaryData_for_Asymmetron_CNE_paper_2016.git, last accessed July 20, 2016).

Physical Distribution and Functional Association of cephalochordate CNEs

For each cephalochordate CNE, we examined its physical position and distance relative to the nearest *B. floridae* gene using a 100-kb maximum distance cutoff. This allowed grouping our cephalochordate CNEs into six classes: intronic,

5′-flanking, 3′-flanking, equidistant (nearest CDSs were found in both 5′- and 3′-flanking directions with equal distance), no flanking (CDSs were found >100 kb away in both 5′- and 3′-flanking directions), and undefined (the flanking region of these CNEs encountered the end of the corresponding scaffold before reaching the 100-kb distance cutoff or any CDS). For the cephalochordate CNEs in the first three classes (intronic, 5′-flanking, and 3′-flanking), we examined the functional annotation of their nearest protein coding genes based on BLAST2GO's annotation (Conesa et al. 2005). We ranked these genes by the number of CNEs that they are associated with and selected the top 5% of this ranked list for examining the enriched gene ontology (GO) terms. To assess statistical significance, Fisher's exact test (Fisher 1922) with false discovery rate (FDR) correction (Benjamini and Hochberg 1995) was used.

Identification of Enriched Motifs in our CNE Sets

We used the *de novo* motif discovery tool HOMER (v4.7) (Heinz et al. 2010) to identify the enriched motifs of our CNE sets. Each discovered motif was searched against the known motif database collected by HOMER to identify its best-matched known motifs.

Manual Annotation for Important Cephalochordate Developmental Genes

Based on previous developmental biology studies on cephalochordates, we selected 50 important cephalochordate developmental genes (i.e. 12 *Hox* genes [*Hox1-Hox10* and *Hox12-Hox13–Hox11* is partially missing in the *B. floridae* v2.0 assembly], 5 *Parahox* genes [*EvxA*, *EvxB*, *Mox*, *Cdx*, *Gsx–Xlox/Pdx* is missing in the *B. floridae* v2.0 assembly], and 33 other genes [*ADMP/SPTSSB*, *Ap2*, *BMP2/4*, *Brachyury*, *Bsx*, *Chordin*, *Engrailed*, *FoxA1*, *FoxA2/HNF3*, *FoxD*, *FoxG1*, *Gbx*, *Gli*, *Hedgehog*, *Id*, *Msx*, *MyoD*, *Nanos*, *Nk2.1*, *Nk2.2*, *Nk2.3/4/5*, *Nodal*, *Otx*, *Pax1/9*, *Pax2/5/8*, *Pax3/7*, *Pax6*, *Pitx*, *SoxE*, *Tbx1/10*, *Tbx2/3*, *Wnt1*, and *ZNF503/703*]). We manually annotated these genes in the *B. floridae* reference assembly (v2.0) with BLAST. The protein domain composition of our annotated genes was further verified by Pfam v27.0 (http://pfam.xfam.org, last accessed July 20, 2016).

Orthologous CNEs in Vertebrates

To investigate the evolution of cephalochordate CNEs associated with those important amphioxus developmental genes within chordates, for each of the CNEs associated with those 50 genes, we used Lastz (v1.02) (Harris 2007) to conduct genome-wide searches in seven well-annotated vertebrates: elephant shark (*Callorhinchus milii*), zebrafish (*Danio rerio*), fugu (*Takifugu rubripes*), frog (*Xenopus tropicalis*), chicken (*Gallus gallus*), mouse (*Mus musculus*), and human (*Homo sapiens*). The genome assemblies (repeat soft-masked version) and gene annotations (in the gene transfer format [GTF]) of elephant shark were downloaded from http://esharkgenome.imcb.a-star.edu.sg/ (last accessed July 20, 2016), and those of all the other species were downloaded from Ensembl (Release 74). We masked the CDS regions of these genomes according to the gene annotations described in those GTF files before the search.

We used a combination of rather low thresholds (hspthresh = 1,500, gappedthresh = 2,500) in Lastz to maximize the sensitivity of our search. A following filter of identity ≥ 65% and the entropy score ≥ 1.7 were adopted to filter out most dubious alignments. The entropy score was calculated in the same way as proposed by Hiller et al. (2012):

Equation 1 for calculating sequence alignment entropy based on Hiller et al. 2012

$$\sum_{b\in\{A,T,G,C\}} \frac{\#\ of\ matches\ f\ or\ b\ in\ the\ alignment}{\#\ of\ total\ matches\ in\ the\ alignment} \cdot \log_2 \frac{\#\ of\ matches\ f\ or\ b\ in\ the\ alignment}{\#\ of\ total\ matches\ in\ the\ alignment}$$

Finally, we applied a stringent syntenic check to filter out those alignments for which the orthology relationships were uncertain. We manually inspected the orthologous relationship for the nearest gene of the cephalochordate query and its Lastz hits in those vertebrate genomes. For each cephalochordate CNE query, we only retained those query-hit pairs that are associated with the same orthologous developmental genes. The true orthologous vertebrate CNE hits and the corresponding cephalochordate CNE query were extracted from their respective genomes with 100-bp flanking regions at both 5′- and 3′-sides. These extracted orthologous cephalochordate-vertebrate CNEs sequences were aligned by MAFFT (v7.0) (Katoh and Standley 2013) using the "L-INS-i" strategy and visualized in Jalview (Waterhouse et al. 2009). The core CNEs were subsequently extracted based on the alignment sequence identity conservation profile provided by Jalview.

Comparison with Previous Studies

Each *B. floridae* CNE or regulatory element previously identified was searched against the *B. floridae* v2.0 assembly using Exonerate (v2.2.0) (Slater and Birney 2005). We also built the LiftOver chain file to facilitate automatic genomic coordinate conversion between the *B. floridae* v1.0 assembly and v2.0 assembly using UCSC's Kent utilities.

Three-Way VISTA Plot

For the genomic regions around *ADMP*, *BMP2/4*, *Brachyury*, *Mox*, and *Msx* genes, we made three-way VISTA plots for *B. floridae*, *B. belcheri*, and *A. lucayanum* with *B. floridae* as the reference. The genome assembly for *B. belcheri* was obtained from http://mosas.sysu.edu.cn/genome/download_data.php (last accessed July 20, 2016). We located the genomic coordinates of these five genes in *B. floridae* based on our manual annotation and found their orthologous counterparts

in *B. belcheri* and *A. lucayanum* using Exonerate (v2.2.0) (Slater and Birney 2005). The genomic regions were then retrieved with 3–5 kb 5′ and 3′ flanking regions. We aligned the sequences by FSA (v1.15.9) (Bradley et al. 2009) and used VISTA (v1.4.26) (Frazer et al. 2004) to visualize sequence conservation profile based on the criteria of 45-bp sliding window and 90% identity cutoff.

Zebrafish Transgenic Experiment

The CNE sequences were amplified from *B. floridae* genomic DNA using primers listed in supplementary table S9 and introduced into the ZED vector upstream of the minimal *gata2a* promoter and EGFP. To control for the efficiency of transgenesis *in vivo*, the reporter genes contained a second cassette composed of a cardiac actin promoter driving the expression of a red fluorescent protein (DsRed). EGFP and DsRed transcriptional units in the ZED vector are separated by an insulator (Bessa et al. 2009). For transgenesis, the *Tol2* transposon/transposase method (Kawakami et al. 2004) was used with minor modifications. A mixture containing 30 ng/μl of transposase mRNA, 30 ng/μl of Qiagen column purified DNA, and 0.05% phenol red was injected in the cell of one-cell stage embryos. Embryos were raised at 28.5°C and staged by hours post fertilization. Embryos selected for imaging were anaesthetised with tricaine and mounted in low-melting agarose. Images were taken on Leica SP5 confocal microscope.

Amphioxus (*B. floridae*) Transgenic Experiment

The genomic DNA of Florida amphioxus (*B. floridae*) was isolated by phenol-chloroform extraction from an adult individual cultured in the laboratory. The amphioxus *Msx*-CNE region was amplified from amphioxus genomic DNA by PCR with FastStart Taq DNA Polymerase, dNTPack (Roche Applied Science, Indianapolis, USA), and cloned between the HindIII site and AsiSI site of the reporter construct derived from the 72-1.27 vector containing the minimal promoter of *B. floridae FoxD* (Corbo et al. 1997; Yu et al. 2004). Primers were 5′-gggAAGCTTcaatacaaacgcgctctgtaaaggtc-3′ (forward primer) and 5′-tctGCGATCGCcaatagttccaaaacggtggtagag-3′ (reverse primer). This construct contains the amphioxus *Msx*-CNE region, 593 bp upstream of the ATG start site of amphioxus *FoxD* including the TATA box, CCAAT box, and GC box elements and the first 15 amino acids of the amphioxus *FoxD* coding region upstream of the *LacZ* gene. Methods for microinjection and staining are according to Holland and Yu (2004).

Results

Sequencing, Assembly, and Mapping of the *Asymmetron* Genome

Illumina sequencing of the three genomic libraries of *A. lucayanum* yielded about 351 million paired-end 100-bp reads and 294 million paired-end 90-bp reads from the Aluca4 and Aluca15 library, respectively, and another 285 million paired-end 100-bp from the Aluca39 library. The completeness of the sequencing was evaluated by matching our previous *A. lucayanum* RNA-Seq assemblies to the *A. lucayanum* WGS reads. Of the two RNA-Seq libraries, about 93.37% and 98.43% of the transcriptome contigs had significant hits (BLASTN, e-value $<$ 1E-6) with the WGS reads, indicating that our WGS represented most of the *A. lucayanum* genome.

Using the WGS reads from the Aluca4 and Aluca15 libraries, which are from the same individual animal, we attempted *de novo* whole genome assembly using the software package Platanus (Kajitani et al. 2014). We estimated the genome size of *A. lucayanum* to be approximately 644.45 mb (supplementary fig. S1). Unfortunately, largely owing to the high polymorphism of the *A. lucayanum* genome, the assembled contigs/scaffolds were fragmented. A total of 141,535 scaffolds ($>$1 kb) were obtained, for a combined length of 409.53 mb. The N50 length of these scaffolds is 3,567 bp. Only approximately 60% of *Asymmetron* reads from our previous RNA-seq study (Yue et al. 2014) could be placed into the *Asymmetron* scaffolds (58.47% for asymAD and 60.64% for asym20h), indicating many assembly gaps, in contrast to the $>$90% completeness of raw WGS reads. Nevertheless, this assembly offers a first draft genome sequence of *A. lucayanum*, which will provide the foundation for more complete assemblies based on additional sequencing.

We next mapped the WGS reads from the three *Asymmetron* genomic libraries to the *B. floridae* reference genome (v2.0). The genome-wide average mapping depth was 3.61X with approximately 9.96% of the genome covered by $\geq$5 reads (mapping quality cutoff = 20). For the coding regions (CDS) of the 28,593 *B. floridae* gene models in the v2.0 reference assembly, the average mapping depth is 19.35 with 48.56% of the CDS regions covered by $\geq$5 reads. Even though the mapping depth was good for the mapped region, only about 20% of the *A. lucayanum* reads could be mapped to the *B. floridae* reference genome, which was fairly consistent across all three WGS libraries (Aluca4, Aluca15, and Aluca39). This observation demonstrates considerable divergence between the *Asymmetron* and *Branchiostoma* genomes and indicates a high probability that the conserved noncoding regions between the two species were retained owing to functional constraints.

Identification of Cephalochordate CNEs Shared between *Asymmetron* and *Branchiostoma*

To identify the CNEs shared between *Asymmetron* and *Branchiostoma*, we used two independent approaches: 1) a WGA-based method and 2) a CSRM-based method (fig. 1).

The WGA-based method assumes colinearity or syntenic conservation of CNEs between the species compared, whereas this positional information was largely uncaptured in the CSRM-based method. Thus, the WGA-based method is more stringent and well defined but, given the fragmented genome assembly of *A. lucayanum*, it can miss many CNEs. The CSRM-based method tends to give a more complete result but the conservation levels of those CNEs are less well defined. Not surprisingly, after excluding ncRNAs, the first method yielded fewer CNEs (45,515) than the second (109,410 CNEs) (table 1 and supplementary files S2 and S3). The 45,515 WGA-based CNEs account for 4.02 mb (0.84%) of the *B. floridae* v2.0 reference genome (480.40 mb after excluding the sequencing and assembly gaps in the *B. floridae* reference genome), while the 109,410 CSRM-based CNEs covered 15.51 mb (3.23%) of the reference genome (table 1). We generated another two CNE sets by taking the intersection and the union of the CSRM-based and WGA-based CNE sets, respectively (fig. 1). The intersection set comprises 40,957 CNEs with a cumulative length of 3.67 mb, while the union set contains 113,070 CNEs accounting for 3.30% (15.84 mb) of the *B. floridae* v2.0 reference genome (table 1 and supplementary files S4 and S5). Fig. 2 shows the CNEs around the *Msx* gene using the *B. floridae* v2.0 assembly as the genomic coordinate reference. Outside of the coding regions, there are several conserved regions; of particular note is the block downstream of the 3′ untranslated region (3′-UTR), which we experimentally verified to be a functional CNE (see below).

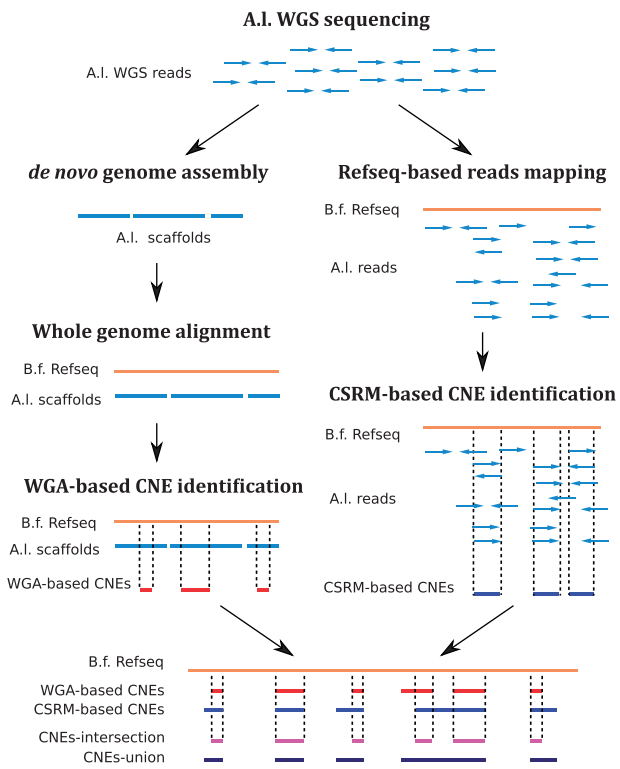

Fig. 1.—A diagram to show the two parallel strategies used in this study for CNE identification. Starting from the raw reads, a whole genome assembly of *A. lucayanum* was generated and further aligned to the *B. floridae* reference genome for CNE identification. We refer CNEs identified by this way as whole-genome alignment-based CNEs (WGA-based CNEs). Alternatively, another CNE set was generated by directly mapping the *A. lucyanuam* reads to the *B. floridae* reference genome and we refer these CNEs as cross-species reads mapping-based CNEs (CSRM-based CNEs). The intersection and union of WGA-based CNEs and CSRM-based CNEs sets were also extracted.

Cephalochordate CNEs are Enriched in the Proximity of *trans*-dev Genes

CNEs typically function as *cis*-regulatory elements and tend to cluster in introns or in the immediate proximity of transcription factors or signaling genes involved in developmental processes ("trans-dev" genes) (Bejerano et al. 2004; Woolfe et al. 2005; Vavouri et al. 2006; Vavouri et al. 2007). Therefore, we investigated the distribution of our identified cephalochordate CNEs as well as their nearest genes (supplementary files S2–S5) within a 100-kb radius using the *B. floridae* genome as the reference. Because the UTRs of most *B. floridae* genes are currently unknown, we marked the boundary of each *B. floridae* gene by its start and stop codons and defined the 100-kb upstream region from the start codon as the 5′-flanking region, and the 100-kb downstream region from the stop codon as 3′-flanking region.

By the above definitions, 41–46% of cephalochordate CNEs are located in introns, while 29–32% and 25–27% are located in 5′ and 3′-flanking regions, respectively (supplementary table S1). Very few (approximately 0.01%) cephalochordate CNEs are equidistant from upstream and downstream neighboring genes. The remaining few CNEs (<1%) are either outside of the 100-kb radius or their

Table 1
Summary of cephalochordate CNEs identified in this study

CNE set	Sequence number	Accumulated length	Mean length	Median length	Maximum length
WGA-based CNEs	45,515	4.02 Mb	88.26 bp	66.00 bp	1,524.00 bp
CSRM-based CNEs	109,410	15.51 Mb	141.73 bp	106.00 bp	3,161.00 bp
CNEs-intersection	40,957	3.67 Mb	89.50 bp	67.00 bp	1,524.00 bp
CNEs-union	113,070	15.84 Mb	140.05 bp	104.00 bp	3,161.00 bp

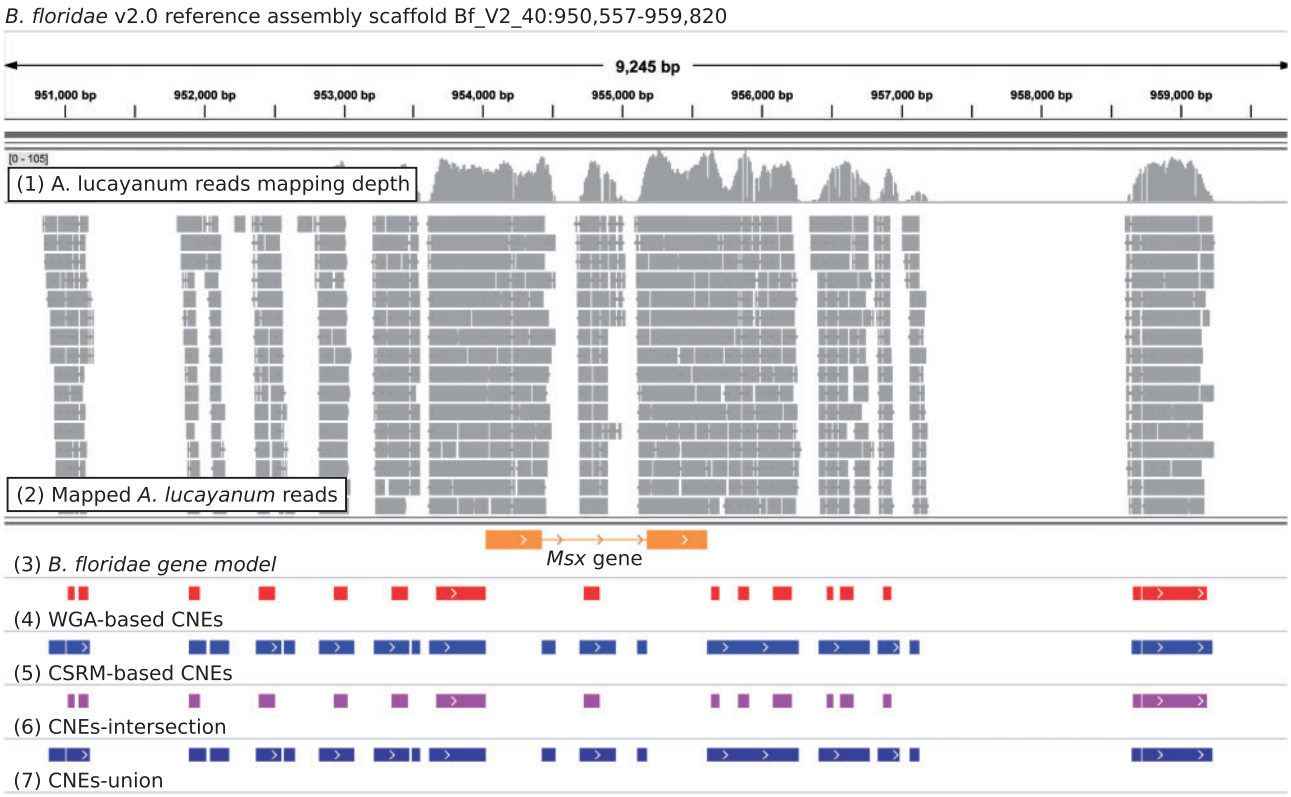

Fig. 2.—An example of the cephalochordate CNEs identified in this study. The *B. floridae Msx* gene (*B. floridae* gene model ID = 278777). The genomic coordinates on the top of the figure show the location (Bf_V2_40:950,557-959,820) of this region according to the *B. floridae* reference assembly. Seven tracks are shown underneath: 1) *A. lucayanum* reads mapping depth, 2) mapped *A. lucayanum* reads, 3) *B. floridae* gene model, 4) WGA-based CNEs, 5) CSRM-based CNEs, 6) the intersection of WGA-based and CSRM-based CNEs, and 7) the union of WGA-based and CSRM-based CNEs. On the mapped reads track, each gray block represents a mapped *A. lucayanum* read with mapping quality ≥20. On the *B. floridae* gene model track, the orange blocks represent the CDS region and the orange line represents the intronic region, whereas the arrows represent the transcription direction of the corresponding gene. On the cephalochordate CNE tracks, each block represents an individual CNE that we identified in this study.

neighboring genes cannot be identified because the scaffold boundary was reached before any genes were identified within the 100-kb flanking radius. For those CNEs located in the 5′ and 3′ gene flanking regions, there was a strong pattern of CNE enrichment immediately adjacent the target genes (supplementary figs S2 and S3). Because of their proximity to coding regions, many of the CNEs probably represent *cis*-regulatory elements, although those within 1 kb of the start and stop codons are likely in 5′- or 3′-UTRs and may include binding sites for proteins initiating transcription or miRNAs in addition to *cis*-acting ncRNAs (Guil and Esteller 2012). We next asked what types of *B. floridae* genes are frequently associated with our identified CNEs. We ranked the genes by the number of CNEs they are associated with. The top 5% chiefly included genes involved in regulatory functions and developmental processes (table 2 and supplementary tables S2–S4). In particular, some genes such as those encoding Bruno4/6, Pax2, TIF1-alpha, and Neurexin-1-beta are associated with >100 CNEs, suggesting considerable evolutionary constraints surrounding these genes (table 3 and supplementary table S5–S7).

Enriched Transcription Factor Binding Motifs in Cephalochordate CNEs

After excluding the low-complexity motifs and other potential false positives, comparing the motifs enriched in our cephalochordate CNE sets to previously characterized binding motifs of various transcription factors yielded 29 enriched motifs in the WGA-based CNE set, 32 in the CSRM-based CNE set, 30 in the CNEs-intersection set, and 36 in the CNEs-union set (supplementary table S5–S8). These enriched motifs matched the binding motifs of several transcription factors including homeobox, basic helix-loop-helix, Zinc finger, and basic region-leucine zipper factors. These genes included *Atf2*, *Esrrb*, *E2f*, *Ebf1*, *FoxO3*, *Nrf*, *Pbx3*, *Pit1*, *Ptf1a*, and *Yy1* (supplementary table S5–S8). This suggests that many, if not most, of the identified cephalochordate CNEs bind transcription factors.

Table 2

Enriched Gene Ontology (GO) terms for the genes associated with most CNEs based on the CNEs-union set

GO-ID	Term	Category	FDR
GO:0048468	Cell development	P	1.46E-63
GO:0048869	Cellular developmental process	P	2.86E-56
GO:0030154	Cell differentiation	P	2.16E-54
GO:0022008	Neurogenesis	P	2.49E-51
GO:0048699	Generation of neurons	P	1.95E-49
GO:0030182	Neuron differentiation	P	1.86E-46
GO:0007399	Nervous system development	P	9.71E-46
GO:0009653	Anatomical structure morphogenesis	P	1.01E-45
GO:0048856	Anatomical structure development	P	1.99E-40
GO:0030030	Cell projection organization	P	2.00E-39

Note.—The highlighted GO terms are shown as top 10 enriched GO terms based on all of our four CNE sets. For the GO term category column, "C" stands for cellular component, "F" for biological function, and "P" biological process. The statistical significance was assessed by Fisher's exact test with FDR correction.

Table 3

Cephalochordate genes associated with most CNEs based on the CNEs-union set

B. floridae gene ID	CNE count	Gene product description
89423	190	Bruno 4/6
56669	173	Paired box protein Pax-2
84482	171	Transcription intermediary factor 1-alpha (TIF1-alpha)
96723	145	Unknown
201173	137	Protein CBFA2T1-like
89425	126	UPF0676 protein C1494.01-like
68413	125	Fibrinogen C domain-containing protein 1-like
281312	121	Receptor-type tyrosine-protein phosphatase delta-like
208446	119	Neurexin-1-beta-like
84479	119	Disks large homolog 5-like

Note.—The highlighted genes are shown as top 10 genes associated with most CNEs based on all of our four CNE sets. The gene descriptions were retrieved based on BLASTP against NCBI nr database.

Highly Conserved Cephalochordate CNEs Shared with Vertebrates

Given that cephalochordates and vertebrates shared a common ancestor >520 mya, we would expect at least some of our identified cephalochordate CNEs to also be conserved in vertebrates. As a proof of concept, for cephalochordate CNEs (from our CNEs-union set) associated with 50 important cephalochordate developmental genes, which include 12 *Hox* genes (*Hox*1-*Hox*10 and *Hox*12-*Hox*13—*Hox*11 is partially missing in the *B. floridae* v2.0 assembly), 5 *Parahox* genes (*EvxA*, *EvxB*, *Mox*, *Cdx*, *Gsx*—*Xlox*/*Pdx* is missing in the *B. floridae* v2.0 assembly), and 33 other genes (*ADMP*/*SPTSSB*, *Ap2*, *BMP2*/*4*, *Brachyury*, *Bsx*, *Chordin*, *Engrailed*, *FoxA1*, *FoxA2*/*HNF3*, *FoxD*, *FoxG1*, *Gbx*, *Gli*, *Hedgehog*, *Id*, *Msx*, *MyoD*, *Nanos*, *Nk2.1*, *Nk2.2*, *Nk2.3*/*4*/*5*, *Nodal*, *Otx*, *Pax1*/*9*, *Pax2*/*5*/*8*, *Pax3*/*7*, *Pax6*, *Pitx*, *SoxE*, *Tbx1*/*10*, *Tbx2*/*3*, *Wnt1*, and *ZNF503*/*703*), we preformed synteny checks to search for their orthologs in seven vertebrates (elephant shark, zebrafish, fugu, frog, chicken, mouse, and human) (See Methods section). One *Hox4*-CNE, one *Gbx*-CNE, one *Msx*-CNE, two *Tbx2*/*3*-CNEs, and three *Znf503*/*703*-CNEs were highly conserved with our sampled vertebrates (table 4 and supplementary figs S4–S11). We examined these eight CNEs using Ensembl (http://www.ensembl.org/, last accessed July 20, 2016) and the UCSC genome browser (http://genome.ucsc.edu/index.html, last accessed July 20, 2016) based on the well-annotated human genome (GRCh37/hg19). We found that the *Hox4*-CNE (*Hox4*-CNE-1) should be a 5′-UTR, whereas the other CNEs evidently have bona fide *cis*-regulatory functions, as suggested by several epigenomic signatures annotated by The Encode Project (The ENCODE Project Consortium 2007). Furthermore, the *Msx*-CNE (*Msx*-CNE-1), 5′ of the coding sequence, and one *ZNF503*/*703*-CNE (*ZNF503*/*703*-CNE-1) have been experimentally verified by previous studies (Holland et al. 2008; Hufton et al. 2009; Royo et al. 2011; Clarke et al. 2012). Finally, for all of these eight cephalochordate-vertebrate CNEs, we found that the sequence conservation between the two cephalochordates (*A. lucayanum* and *B. floridae*) clearly extends beyond the core CNE regions, echoing the trend previously observed in vertebrates (McEwen et al. 2009; Maeso and Tena 2016) that flanking sequences of ancient CNEs tend to be more conserved between more closely related lineages.

Previously Verified *Branchiostoma cis*-Regulatory Elements Are Largely Conserved with *Asymmetron*

We compared the CNEs shared between *A. lucayanum* and *B. floridae* with the 30 amphioxus (25 in *B. floridae* and 5 in *B. lanceolatum*) regulatory elements previously verified in reporter assays (Manzanares et al. 2000; Yu et al. 2004; Wada et al. 2006; Beaster-Jones et al. 2007; Holland et al. 2008; Royo et al. 2011; Clarke et al. 2012; Irimia et al. 2012a; Maeso et al. 2012; Van Otterloo et al. 2012; Acemel et al. 2016). Twenty-six of these 30 can be mapped to the version 2.0 assembly of *B. floridae*; presumably the absence of the other four is owing to errors in the assembly, which represents a single composite allele, whereas version 1.0 of the *B. floridae* genome used by Hufton et al. (2009) includes both alleles. Of these 26 functional elements 20 (76.92%) were also present in our WGA-based CNE set and in the CNEs-intersection set, and 24 (92.30%) were in our CSRM-based CNE set and CNEs-union set (table 5). The two CNEs that we missed are one *Elav*-like CNE at Bf_V2_69:357679-357729 and one *Irx*-*Sowah* 9d CNE at Bf_V2_14:300101-300634. However, we did find two other CNEs located close to these genes (3 bp and 27 bp away, respectively), suggesting that we might still recover the potential functionally important regions represented by these two CNEs. For those CNEs matched with previously

Table 4
The genomic coordinates of eight cephalochordate CNEs that are also conserved in vertebrates

CNE	Species	Assembly version	Chromosome/scaffolds	Start	End	Strand
Hox4-CNE-1	*B. floridae*	JGI v2.0	Bf_V2_12	935683	935734	+
	C. milii	v6.1.3	scaffold_14	5156972	5157024	+
	C. milii	v6.1.3	scaffold_79	1146070	1146121	+
	D. rerio	Zv9	chr23	36182558	36182606	+
	T. rubripes	FUGU4	scaffold_66	127864	127912	-
	X. tropicalis	JGI v4.2	GL172692.1	1443781	1443838	+
	X. tropicalis	JGI v4.2	GL172862.1	463024	463072	+
	G. gallus	Galgal4	chr2	32825928	32825980	-
	G. gallus	Galgal4	chr7	15779237	15779290	-
	M. musculus	GRCm38	chr2	74727226	74727278	+
	M. musculus	GRCm38	chr6	52191689	52191741	-
	M. musculus	GRCm38	chr15	103034674	103034722	+
	H. sapiens	GRCh37	chr2	177016308	177016361	+
	H. sapiens	GRCh37	chr7	27170353	27170406	-
	H. sapiens	GRCh37	chr12	54447658	54447706	+
Gbx-CNE-1	*B. floridae*	JGI v2.0	Bf_V2_98	338705	338749	+
	D. rerio	Zv9	chr24	35438769	35438813	-
	T. rubripes	FUGU4	scaffold_107	110492	110536	+
	X. tropicalis	JGI v4.2	GL172651.1	1936474	1936517	-
	X. tropicalis	JGI v4.2	GL172651.1	1942293	1942336	+
	G. gallus	Galgal4	chr2	173160	173204	+
	M. musculus	GRCm38	chr5	24526927	24526971	-
	H. sapiens	GRCh37	chr7	150864986	150865030	-
Msx-CNE-1	*B. floridae*	JGI v2.0	Bf_V2_40	953325	953435	+
	C. milii	v6.1.3	scaffold_3	13863219	13863320	-
	C. milii	v6.1.3	scaffold_53	4190366	4190495	-
	D. rerio	Zv9	chr14	168407	168543	+
	T. rubripes	FUGU4	scaffold_116	868022	868152	+
	T. rubripes	FUGU4	scaffold_3613	3253	3383	+
	X. tropicalis	JGI v4.2	GL173077.1	691910	692039	+
	G. gallus	Galgal4	chr4	78386959	78387088	+
	M. musculus	GRCm38	chr5	37826828	37826956	-
	H. sapiens	GRCh37	chr4	4858647	4858775	+
Tbx2/3-CNE-1	*B. floridae*	JGI v2.0	Bf_V2_147	3548171	3548268	+
	C. milii	v6.1.3	scaffold_47	3346941	3347032	-
	D. rerio	Zv9	chr5	57923023	57923117	+
	D. rerio	Zv9	chr5	75416575	75416677	-
	D. rerio	Zv9	chr15	26713164	26713258	-
	T. rubripes	FUGU4	scaffold_84	934772	934875	+
	X. tropicalis	JGI v4.2	GL172708.1	2281836	2281930	-
	X. tropicalis	JGI v4.2	GL173091.1	420790	420895	-
	G. gallus	Galgal4	chr15	12206709	12206815	-
	G. gallus	Galgal4	chr19	7638979	7639073	+
	M. musculus	GRCm38	chr5	119670890	119670994	-
	M. musculus	GRCm38	chr11	85832678	85832773	-
	H. sapiens	GRCh37	chr12	115122004	115122108	+
	H. sapiens	GRCh37	chr17	59477114	59477209	-
Tbx2/3-CNE-2	*B. floridae*	JGI v2.0	Bf_V2_147	3549098	3549149	+
	D. rerio	Zv9	chr5	57923920	57923971	-
	D. rerio	Zv9	chr15	26712039	26712091	-
	T. rubripes	FUGU4	scaffold_300	238408	238461	+
	T. rubripes	FUGU4	scaffold_300	243979	244032	+
	X. tropicalis	JGI v4.2	GL172708.1	2280047	2280099	-

(continued)

Table 4 Continued

CNE	Species	Assembly version	Chromosome/scaffolds	Start	End	Strand
	X. tropicalis	JGI v4.2	GL173091.1	419230	419282	-
	G. gallus	Galgal4	chr15	12205007	12205059	-
	M. musculus	GRCm38	chr5	119669212	119669264	-
	H. sapiens	GRCh37	chr12	115123879	115123931	+
Znf503/703-CNE-1	*B. floridae*	JGI v2.0	Bf_V2_167	2385480	2385629	+
	C. milii	v6.1.3	scaffold_3	13121560	13121704	+
	D. rerio	Zv9	chr5	26009609	26009746	-
	D. rerio	Zv9	chr13	17515432	17515575	+
	T. rubripes	FUGU4	scaffold_7	2065877	2066001	-
	T. rubripes	FUGU4	scaffold_86	79136	79279	-
	X. tropicalis	JGI v4.2	GL172676.1	1844110	1844257	-
	X. tropicalis	JGI v4.2	GL172901.1	202622	202765	-
	G. gallus	Galgal4	chr6	14130380	14130523	+
	M. musculus	GRCm38	chr8	26961370	26961507	+
	M. musculus	GRCm38	chr14	21991346	21991490	-
	H. sapiens	GRCh37	chr8	37532872	37533008	+
	H. sapiens	GRCh37	chr10	77165028	77165172	-
Znf503/703-CNE-2	*B. floridae*	JGI v2.0	Bf_V2_167	2387049	2387137	+
	C. milii	v6.1.3	scaffold_3	13125570	13125657	+
	D. rerio	Zv9	chr13	17516606	17516696	+
	T. rubripes	FUGU4	scaffold_86	78313	78398	-
	X. tropicalis	JGI v4.2	GL172901.1	199576	199665	-
	M. musculus	GRCm38	chr14	21988662	21988751	-
	H. sapiens	GRCh37	chr10	77162348	77162437	-
Znf503/703-CNE-3	*B. floridae*	JGI v2.0	Bf_V2_167	2387253	2387382	+
	C. milii	v6.1.3	scaffold_3	13125892	13126016	+
	D. rerio	Zv9	chr13	17517345	17517461	+
	T. rubripes	FUGU4	scaffold_86	77609	77725	-
	X. tropicalis	JGI v4.2	GL172901.1	193902	194019	-
	M. musculus	GRCm38	chr14	21987870	21987987	-
	H. sapiens	GRCh37	chr10	77161518	77161635	-

verified regulatory elements, we found that their sequences tend to be generally longer than those non-matched CNEs (Wilcoxon rank sum test, *P*-value = 1.849E-3 for WGA-based CNEs and *P*-value = 5.485E-12 for CSRM-based CNEs), but no statistical difference was found in sequence identity between *A. lucayanum* and *B. floridae* (Wilcoxon rank sum test, *P*-value = 0.9154 for WGA-based CNEs; sequence identity for CSRM-based CNEs is not readily calculable).

The Number of CNEs Identified is Highly Dependent on the Method

There are three previous genome-wide studies identifying CNEs shared between *Branchiostoma sp.* and vertebrates. Two used the *B. floridae* v1.0 assembly. Putnam et al. (2008) identified 77 CNEs based on *B. floridae* versus human, while Hufton et al. (2009) identified 1,299 CNEs based on *B. floridae* versus mouse, Fugu, and zebrafish. After removing redundancies by mapping these CNEs to the *B. floridae* v2.0 assembly and removing those overlapping with CDS regions or ncRNAs, 54 and 669 CNEs, respectively, were left. However, our CNEs-union set matched only 21 of these 54 CNEs (identified by Putnam et al. 2008) and just 120 of those 669 CNEs (identified by Hufton et al. 2009). Surprisingly, only 6 of the 54 CNEs in the first set are also in the second set, even though both compared cephalochordates and vertebrates. We think this large discrepancy likely comes from the differences in methodology and conservation criteria. In the study by Putnam et al. (2008), a WGA-based method similar to ours was used, with the criterion of 60% nucleotide identity across a 50-bp window, whereas Hufton et al. (2009) used a local-similarity-based method centered on conserved gene families. Also for the Hufton et al. (2009) study, a later review pointed out that the authors might have overestimated the CNEs shared between cephalochordates and vertebrates given that they did not check the detailed position and orientation of those CNEs relative to their respective target genes (Maeso et al. 2013).

The third study compared the Chinese amphioxus, *B. belcheri*, with *B. floridae* and vertebrates (human and opossum) using a combination of Lastz-ChainNet-based and BLASTN-based methods. It found at least 135,046 CNEs shared

Table 5
Comparison between previously experimentally verified *B. floridae* CNEs or regulatory elements (REs) and this study

Functional *B. floridae* CNE/RE name	Genomic coordinate (in the *B. floridae* v2.0 assembly)	Literature source	Comparison with this study			
			WGA-based CNEs	CSRM-based CNEs	CNEs-intersection	CNEs-union
Elav-like CNE[a]	Bf_V2_69:357679-357729	Hufton et al. (2009)	X	X	X	X
Engrailed RE	Bf_V2_9:1267978-1274277	Beaster-Jones et al. (2007)	✓	✓	✓	✓
EvxA? RE 2473	Bf_V2_12:378112-378330	Acemel et al. (2016)	✓	✓	✓	✓
FoxD RE	Bf_V2_113:901685-902885	Yu et al. (2004)	✓	✓	✓	✓
Hedgehog RE	Bf_V2_205:188300-193172	Irimia et al. (2012a)	✓	✓	✓	✓
Hox1A RE	Bf_V2_12:999003-1001503	Manzanares et al. (2000); Wada et al. (2006)	✓	✓	✓	✓
Hox2B RE	Bf_V2_12:986507-990914	Manzanares et al. (2000); Wada et al. (2006)	✓	✓	✓	✓
Hox2C RE	Bf_V2_12:980069-981704	Manzanares et al. (2000); Wada et al. (2006)	✓	✓	✓	✓
Hox3B RE	Bf_V2_12:977525-979277	Manzanares et al. (2000); Wada et al. (2006)	✓	✓	✓	✓
Hox1 1655 RE	Bf_V2_12:1119489-1119959	Acemel et al. (2016)	✓	✓	✓	✓
Hox1 1739 RE	Bf_V2_12:1060551-1060880	Acemel et al. (2016)	✓	✓	✓	✓
Hox1 1784 RE	Bf_V2_12:1018545-1019524	Acemel et al. (2016)	✓	✓	✓	✓
Hox1 1801 RE	Bf_V2_12:1002265-1002697	Acemel et al. (2016)	✓	✓	✓	✓
Irx-Sowah 1a CNE	Bf_V2_14:276485-278804	Maeso et al. (2012)	✓	✓	✓	✓
Irx-Sowah 5b CNE	Bf_V2_14:351877-352857	Maeso et al. (2012)	X	✓	X	✓
Irx-Sowah 6a CNE	Bf_V2_14:424282-425437	Maeso et al. (2012)	X	✓	X	✓
Irx-Sowah 6c CNE	Bf_V2_14:315985-317211	Maeso et al. (2012)	X	✓	X	✓
Irx-Sowah 9d CNE[a]	Bf_V2_14:300102-300634	Maeso et al. (2012)	X	X	X	X
Irx-Sowah 10b CNE	Bf_V2_14:378423-380890	Maeso et al. (2012)	X	✓	X	✓
Irx-Sowah 10d CNE	Bf_V2_14:301002-303621	Maeso et al. (2012)	✓	✓	✓	✓
Msx CNE	Bf_V2_40:953259-953496	Hufton et al. (2009); Royo et al. (2011); Clarke et al. (2012)	✓	✓	✓	✓
Six3/6 CNE	Bf_V2_245:211307-211352	Hufton et al. (2009); Royo et al. (2011)	✓	✓	✓	✓
SoxB2 CNE	Bf_V2_196:4387592-4387942	Hufton et al. (2009); Royo et al. (2011)	✓	✓	✓	✓
SoxE RE	Bf_V2_174:2742068 2744567	Van Otterloo et al. (2012)	✓	✓	✓	✓
Sp5 CNE	Bf_V2_149:861774-862000	Hufton et al. (2009)	✓	✓	✓	✓
ZNF503/703 CNE	Bf_V2_167:2385491-2385650	Holland et al. (2008); Royo et al. (2011); Clarke et al. (2012)	✓	✓	✓	✓

[a]Although there is no direct overlap between our CNEs and these two regions, we found other CNEs in the immediate proximity of these regions.

between *B. floridae* and *B. belcheri*, with 1,084 also shared with vertebrates (Huang et al. 2014). Because this result is based on their *B. belcheri* reference coordinate system and not on *B. floridae*, it was not straightforward to compare their results with ours. Therefore, using the same criteria that we used for the *Asymmetron–Branchiostoma* comparison, we ran our WGA-based CNE pipeline to generate our own CNE set shared between these two *Branchiostoma* species. This resulted in 179,224 CNEs with a cumulative length of 16.48 Mb, which is considerably more than the CNEs-union set we obtained for the *Asymmetron–Branchiostoma* comparison (CNE count: 113,070; cumulative length: 15.84 Mb). Most of the *A. lucayanum–B. floridae* CNEs (77.32% when calculating based on the CNEs-union set) were recapitulated in the *B. floridae–B. belcheri* CNE set. Moreover, for these shared CNEs across all three amphioxus species, the comparison between the two *Branchiostoma* species reveals longer sequence conservation tracts than the comparison between *Asymmetron* and *Branchiostoma* under the same criteria (Wilcoxon rank sum test, P-value $< 2.2E-16$). The same trend holds for those ancient CNEs that are shared between cephalochordate and vertebrates. All of these observations are

consistent with what we would expect based on the phylogenetic relationship among these three cephalochordate species. Chances are that many of these 180,000 CNEs shared between *B. belcheri* and *B. floridae* are not gene regulatory elements. These two congeners diverged about 100 mya (Nohara et al. 2005). However, as cephalochordates are evolving particularly slowly (Yue et al. 2014), 100 mya appears to be insufficient for meaningful CNEs identification in cephalochordate genomes.

Experimental Verification of *in silico* CNEs in Zebrafish and Amphioxus

To verify that some of the CNEs that were identified computationally really are functional *cis*-regulatory elements, we generated Vista alignments between *B. floridae* and *B. belcheri* and between *B. floridae* and *A. lucayanum* for five genes (*ADMP*, *BMP2/4*, *Brachyury*, *Mox*, and *Msx*) (fig. 3). As this figure shows, the Vista alignments for the two *Branchiostoma* species reveal altogether too much conservation outside the coding regions. Therefore, for each of these genes, we randomly selected a noncoding region conserved between *A. lucayanum* and *B. floridae* as well as with *B. belcheri* (boxed in fig. 3) to test experimentally by linking them to reporter constructs. For *ADMP* and *BMP2/4*, so many regions are conserved between the two genera that our selection was somewhat arbitrary. All reporter constructs were injected into zebrafish eggs and, for the *Msx 3′* CNE, into *B. floridae* eggs as well (supplementary table S9; fig. 4). As injections into amphioxus eggs are time-consuming, we did not attempt to express the other constructs in amphioxus. The *Msx* CNE downstream of the 3′ UTR has a central region of 11 bp that is not conserved; therefore, while it could be considered to be two CNEs in our *in silico* CNE identification, the entire region was tested in expression assays.

All of the cephalochordate CNEs directed tissue-specific expression in zebrafish, while the 3′ *Msx*-CNE also directed expression in amphioxus (fig. 4). The amphioxus *ADMP*-CNE directs expression throughout much of the zebrafish shield at 90% epiboly (fig. 4A). This domain is somewhat broader than expression of the native zebrafish *ADMP* gene at the same stage (Dickmeis et al. 2001). Expression driven by the *BMP2/4* CNE recapitulates the expression pattern of the native genes in both zebrafish and amphioxus at the gastrula stage—broadly in both ectoderm and mesendoderm (fig. 4C). The amphioxus *Brachyury* CNE recapitulates native expression of the zebrafish *Brachyury* in the notochord (fig. 4E) (Schulte-Merker et al. 1994). The native *Brachyury* gene is also expressed in the amphioxus notochord (Holland et al. 1995). The amphioxus *Mox* CNE directs expression to developing muscle in zebrafish (fig. 4G). *Mox* is expressed in developing muscle in both amphioxus (Minguillón and Garcia-Fernàndez 2002) and in *Xenopus*, as well as in other mesodermal tissues (Candia and Wright 1995). Zebrafish *Mox* orthologs *meox2a* and *meox2* are first expressed at the end of somitogenesis in formed myotomes and later in fin myoblasts and specific muscles of the head (Nguyen et al. 2014). The amphioxus *Msx* CNE directs expression to developing muscle in both amphioxus and vertebrates (fig. 4I-M), one of the two domains that express the native gene (Sharman et al. 1999). The other

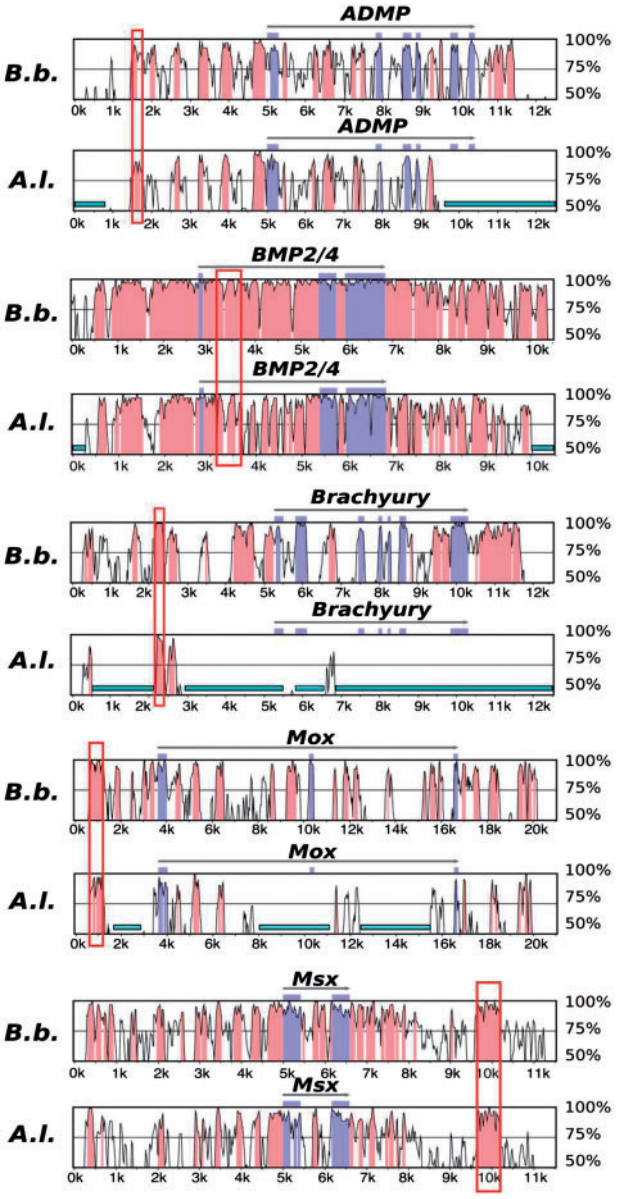

Fig. 3.—Vistaplots reveal high sequence conservation across cephalochordate genomes. The genomic sequences with >50% sequence identity compared with *B. floridae* are shown for *B. belcheri* (denoted as *B. b.*) and *A. lucayanum* (denoted as *A. l.*) around *ADMP, BMP2/4, Brachyury, Mox*, and *Msx* genes. The CDS regions are depicted in blue, while CNEs with 90% identity over 45-bp window are depicted in red. The tested CNE for each gene was highlighted by the red boxes. The cyan bars at the bottom indicate assembly gaps in *A. lucyanuam*.

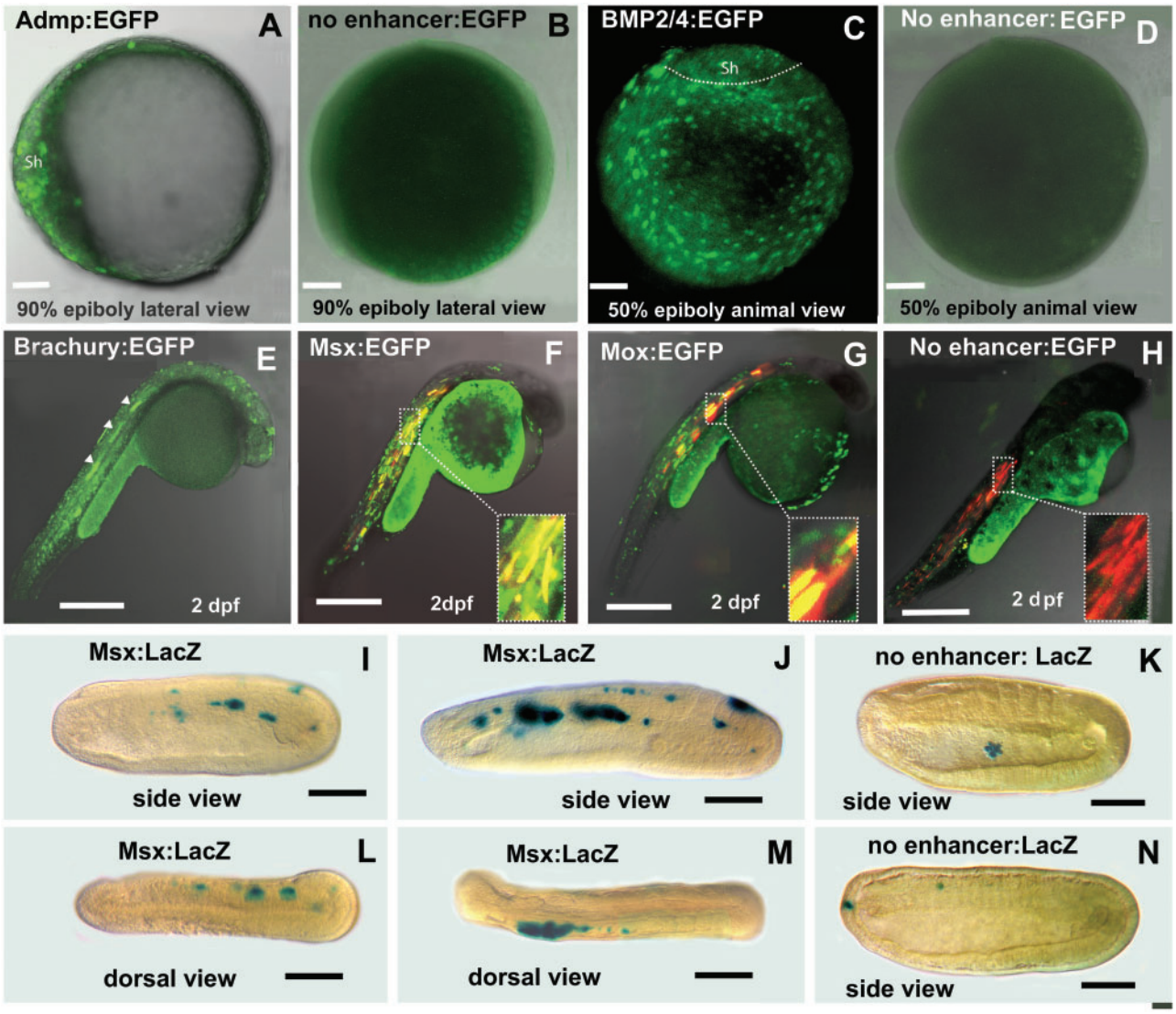

Fig. 4.—Amphioxus CNEs identified *in silico* by comparing cephalochordate genomes are functional enhancers in zebrafish. (A) *ADMP* CNE drives the expression of enhanced green fluorescent protein (EGFP) into dorsal shield of zebrafish late gastrula. (B) Negative control for A shows no expression. (C) EGFP expression driven by *BMP2/4* CNE is present throughout the blastoderm with lower intensity in the shield region at gastrula stage. (D) Negative control for C shows no expression. (E) The activity of the *Brachyury* CNE at late segmentation period. White arrows indicate expression in the notochord. (F) The *Msx* CNE directs expression to the muscles. Red marks expression of DSRED directed by a muscle-specific zebrafish enhancer. Yellow shows co-expression directed by both enhancers in the muscles. (G) The *Mox* CNE from amphioxus directs expression to muscle in the zebrafish. Red marks expression directed by a muscle-specific zebrafish enhancer. Yellow shows co-expression directed by both enhancers in the muscles. (H) Negative control. EGFP expression with no enhancer is nonspecific. Red indicates expression of a co-injected muscle-specific enhancer. (I–N). Amphioxus embryos. Anterior to the left. (I) Mid-neurula. Expression driven by the *Msx*-CNE is mosaic in muscle. (J) Late-neurula. Expression driven by *Msx*-CNE is expressed strongly in muscle. (K) Negative control. Early neurula. Expression limited to a single sick cell in the gut lumen. (L) Dorsal view. Expression of the *Msx*-CNE in muscles on the right side. (M) Dorsal view. Expression driven by the *Msx*-CNE is in muscles on the left side. (N) Negative control. Expression of the empty vector in a single anterior ectodermal cell and in a single cell in the vicinity of the muscles.

domain is in the neural tube. An amphioxus CNE 5′ of the *Msx* coding region was previously shown to direct expression to the neural tube in zebrafish (Hufton et al. 2009). Interestingly, none of the four zebrafish *Msx* genes is expressed in muscle (Akimenko et al. 1995). However, mouse *Msx1* is expressed in limb muscle precursor cells (Bendall et al. 1999). In the invertebrates *Platynereis dumerilli* and *Drosophila melanogaster*, *Msx* is expressed in presumptive myoblasts that give rise to segmental muscles (Jagla et al. 1999; Ramos and Robert 2005; Saudemont et al. 2008).

These results show that comparisons between *Asymmetron* and *Branchiostoma* are highly effective in

revealing functional CNEs. Although the ones we tested functionally were also conserved with vertebrates, it is likely that most of those conserved between the two cephalochordate genera but not vertebrates will also prove to be functional enhancers.

Discussion

The Goldilocks Principle in CNE Identification

When CNEs are identified by comparisons of homologous regions of DNA among different species, the sequences being compared have to be conserved to just the right degree. If they are too divergent, regulatory DNA sequences may have moved in relation to the coding sequence; transcription factor binding sites may have shifted position within the regulatory element; or the sequence may have changed considerably. If, on the other hand, the sequences are too highly conserved, regulatory elements cannot be distinguished from the background nonfunctional DNA.

The effective phylogenetic distance for comparisons of genome sequences to reveal meaningful CNEs depends not only on the divergence time but on the rates of evolution as well. For fast-evolving organisms, the phylogenetic distance must be small, while for slow-evolving ones, the distance between the organisms being compared must be much larger. For example, tunicates are evolving much, much faster than vertebrates and cephalochordates (Tsagkogeorga et al. 2010; Yue et al. 2014). Genome sequence alignments between the tunicate *Ciona intestinalis* and vertebrates revealed few, if any conserved non-coding elements. In contrast, the genetic distance between the tunicates *C. intestinalis* and *Ciona savignyi*, which split 3–4 mya, seems to be about the same as that between human and chicken, which split about 310 mya (Furlong 2005; Irvine 2013). Consequently, like comparisons between humans and chickens and/or frogs, comparisons between the two congeners of *Ciona* have revealed many CNEs (Russo et al. 2004; Irvine 2013). In addition, separate analyses of the genomes of the two *Ciona* species and six vertebrates, revealed 183 CNEs that are syntenic among vertebrates. However, 182 of them were located in non-syntenic positions in tunicate genomes (Sanges et al. 2013).

In contrast with tunicates, comparisons between fairly distant vertebrates, which are evolving relatively slowly, with agnathans splitting from gnathostomes about 450 mya, and mammals first appearing about 320 mya, have revealed numerous CNEs. Comparisons between human and fugu initially revealed about 1,400 CNEs (Woolfe et al. 2005). In addition, of a set of 1,205 human CNEs distributed across about 1% of the human genome, 1,142 were conserved with chicken, 1,035 with fugu, 789 with elephant shark but only 73 with the lamprey (McEwen et al. 2009). This implies that CNEs conserved between amphioxus and vertebrates are probably performing vital functions. Although cephalochordates and vertebrates diverged >520 mya, because cephalochordates are evolving even more slowly than the slowest evolving vertebrate known, the elephant shark (Venkatesh et al. 2014; Yue et al. 2014), hundreds of CNEs that are shared between amphioxus and vertebrates have been identified (Putnam et al. 2008; Hufton et al. 2009; Huang et al. 2014). Some of them are even conserved across greater evolutionary distance (e.g. also conserved in hemichordates and even protostomes or cnidarians; Royo et al. 2011; Clarke et al. 2012; Simakov et al. 2015). To identify more regulatory elements, especially those cephalochordate-specific ones, we compared the two most phylogenetically distant genera of cephalochordates (*Asymmetron* and *Branchiostoma*), which diverged about 120–160 mya. While intra-genus comparisons for very fast-evolving species such as tunicates and relatively fast-evolving ones such as *Drosophila* (Schmid and Tautz 1997; Makunin et al. 2014), which diverged 30–40 mya, have revealed numerous enhancers (>2,000 for *Drosophila*), for very slowly evolving species, comparisons over a much wider phylogenic distance are better. Thus, as fig. 3 shows, for cephalochordates, even the 112 million years of separation for *Branchiostoma* (*B. floridae* and *B. belcheri*) estimated from mitochondrial DNA sequences (Nohara et al. 2005) does not suffice to separate the CNEs from background sequences. Levels of conservation for *ADMP*, *BMP2/4*, *Brachyury*, *Mox*, and *Msx* in the 3–5 kb up- and downstream of the coding regions and in the introns are high between two *Branchiostoma* species, revealing only a few regions with ≤50% identity. This widespread conservation in the noncoding regions of *Branchiostoma* species echoes a previous observation about the *Hedgehog* locus of *Branchiostoma*; the noncoding regions of this locus are strikingly similar among the three *Branchiostoma* species (*B. floridae*, *B. lanceolatum*, and *B. belcheri*; Irimia et al. 2012b). In line with the very slow evolution, conservation between *Branchiostoma* and *Asymmetron* is also fairly high given the 120–160 million years since they diverged (Kon et al. 2007; Yue et al. 2014). Although some of the 113,070 CNEs we identified that are conserved between *A. lucayanum* and *B. floridae* may not be functional regulatory elements, with 23,000 genes in cephalochordates, one would expect to find a minimum of 50,000 regulatory elements. Therefore, in contrast to the species of *Branchiostoma*, the *Asymmetron* versus *Branchiostoma* comparison seems to be better for identifying functional regulatory elements. Remarkably, these two genera will hybridize and develop at least to the mid-larval stage even though they have different numbers of chromosomes (2n = 38 in *B. floridae*; 2n = 34 in *A. lucayanum*) and different sized genomes (480.40 mb after excluding the sequencing and assembly gaps in *B. floridae*; 645 mb in *A. lucayanum*) (Holland et al. 2015). Comparisons between these two genera and their hybrids promise to be highly informative for understanding the genetic mechanisms of development, in general, and the construction of gene regulatory networks in particular.

CNE Evolution

Once CNEs have been identified between one or more groups, comparisons with somewhat more distantly related organisms can show how CNEs have evolved as organisms have diverged. For example, comparisons among mammals have revealed loss of many CNEs in one mammalian lineage or another (Hiller et al. 2012; Villar et al. 2015). CNEs that were not lost in any mammalian lineage were, in general, older than those that were lost. Similarly, comparative genomics revealed several possible enhancers near the *Shh* gene conserved between the coelacanth and some sarcopterygian and actinopterygian fishes and verified in reporter assays (Lang et al. 2010). However, several of these CNEs were missing in more recently evolved sarcopterygian and actinopterygian fishes.

Not only can old enhancers disappear during evolution, if they persist they may retain old functions and/or acquire new functions. Examples of such functional conservation are the *Msx* CNE in the present study and a CNE near the *EBF3* gene in lamprey and human (McEwen et al. 2009). The amphioxus CNE near *ZNF503/703* and its two vertebrate homologs show that CNEs can both retain old functions and acquire new ones in evolution. This amphioxus CNE directs expression to the amphioxus notochord and somites but not to the central nervous system (CNS) and to some, but not all, of the domains that the corresponding enhancers adjacent the human *ZNF503* and *ZNF703* genes direct expression to in the mouse (Holland et al. 2008). Moreover, the amphioxus enhancer directs expression in the mouse to one domain in the eye to which the vertebrate counterparts do not direct expression. Similarly, in vertebrates, some CNEs associated with *GLI3*, which transduces *Shh* signaling, show conserved expression in mouse and zebrafish, while one CNE, which directs expression to the limb bud in the mouse and chick, directs expression to the notochord and blood cell precursors, but not to the limb, in the zebrafish (Anwar et al. 2015). In fact, such examples of acquiring new regulatory functions by co-option or modification of preexisting CNEs are prevalent in the evolution of new regulatory elements (Maeso and Tena 2016).

New regulatory elements can also be gained via exaptation of repetitive elements and transposable elements. For example one family of RSR elements that function as transcriptional enhancers in the strongylocentrotid family of sea urchins evolved from repetitive sequence at the base of that family; RSR elements are absent from other sea urchins such as *Heliocidaris* and *Lytechinus* (Dayal et al. 2004). The co-option of transposable elements for regulatory elements has been well-documented (Britten 1997). An example of how transposable elements may become candidates for new regulatory elements is shown by the amphioxus *FoxD* gene (Yu et al. 2004). We noted a transposable element with many TCF binding sites located about 1 kb upstream of the start codon of the *FoxD* gene in a clone from a genomic library. However, this sequence was not part of the tissue-specific enhancer for this gene and, as it was absent from the same place in the *FoxD* gene in the genome sequenced from another individual, it had not become fixed in the population.

As more genomes become available, it may be informative to investigate the amphioxus CNEs in the context of hemichordates and early-diverged echinoderms. Two noncoding elements associated with the *Pax1/9* gene were found to be conserved among vertebrates, amphioxus and hemichordates (Simakov et al. 2015), raising the question of just when the amphioxus CNEs that we determined in the present study evolved. However, given the different body plans of chordates and ambulacrarians, as well as the rapid turnovers of *cis*-regulatory elements in general, it may be difficult to trace the origins of most amphioxus CNEs in deuterostome evolution.

Supplementary Material

Supplementary files S1–S5, Figures S1–S11, and Tables S1–S11 are available at *Genome Biology and Evolution* online (http://www.gbe.oxfordjournals.org/).

Acknowledgments

We thank Dr Michael Hiller for sharing the script for alignment entropy calculation, Dr Michael H. Kohn for helpful suggestions during manuscript writing, Dr Robert A. Cornell, Dr Peter W. H. Holland, Dr Manuel Irimia, Dr Ignacio Maeso, Dr Matthew Blow, Dr Len A. Pennacchio, and Dr Hiroshi Wada and for providing detailed information about the amphioxus regulatory regions that they identified in their previous studies, Dr. Nicholas D. Holland for collecting the specimens of *A. lucayanum*, Dr Koichi Kawakami and Dr Jose Bessa for the reagents used in zebrafish transgenic experiment, and the anonymous reviewers for their valuable comments that helped us to improve the manuscript. J.X.Y. was supported by a doctoral fellowship from Rice University when conducting this study; he is currently supported by a postdoctoral fellowship from Fondation ARC pour la Recherche sur le Cancer (n°PDF20150602803). L.Z.H. was supported by the grant NSF IOS1353688 from National Science Foundation. I.K. and Z.K. were supported by the grant GC15-21285J from Grantová Agentura České Republiky. J.K.Y. was supported by the Career Development Award AS-98-CDA-L06 from Academia Sinica, Taiwan, and grants 102-2311-B001-011-MY3 and 104-2923-B-001-002-MY3 from the Ministry of Science and Technology (MOST), Taiwan.

Literature Cited

Acemel RD, et al. 2016. A single three-dimensional chromatin compartment in amphioxus indicates a stepwise evolution of vertebrate Hox bimodal regulation. Nat Genet. 48:336–341.

Akimenko MA, Johnson SL, Westerfield M, Ekker M. 1995. Differential induction of four *msx* homeobox genes during fin development and regeneration in zebrafish. Development 121:347–357.

Anwar S, et al. 2015. Identification and functional characterization of novel transcriptional enhancers involved in regulating human *GLI3* expression during early development. Dev Growth Differ. 57: 570–580.

Beaster-Jones L, Schubert M, Holland LZ. 2007. *Cis*-regulation of the amphioxus *engrailed* gene: insights into evolution of a muscle-specific enhancer. Mech Dev. 124:532–542.

Bejerano G, et al. 2004. Ultraconserved elements in the human genome. Science 304:1321–1325.

Bendall AJ, Ding J, Hu G, Shen MM, Abate-Shen C. 1999. *Msx1* antagonizes the myogenic activity of *Pax3* in migrating limb muscle precursors. Development 126:4965–4976.

Benjamini Y, Hochberg Y. 1995. Controlling the false discovery rate: a practical and powerful approach to multiple testing. J R Stat Soc Ser B. 57:289–300.

Bessa J, et al. 2009. Zebrafish enhancer detection (ZED) vector: a new tool to facilitate transgenesis and the functional analysis of *cis*-regulatory regions in zebrafish. Dev Dyn. 238:2409–2417.

Bolger AM, Lohse M, Usadel B. 2014. Trimmomatic: a flexible trimmer for Illumina sequence data. Bioinformatics 30:2114–2120.

Braasch I, et al. 2016. The spotted gar genome illuminates vertebrate evolution and facilitates human-teleost comparisons. Nat Genet. 48:427–437.

Bradley RK, et al. 2009. Fast statistical alignment. PLoS Comput Biol. 5:e1000392.

Britten RJ. 1997. Mobile elements inserted in the distant past have taken on important functions. Gene 205:177–182.

Buenrostro JD, Giresi PG, Zaba LC, Chang HY, Greenleaf WJ. 2013. Transposition of native chromatin for fast and sensitive epigenomic profiling of open chromatin, DNA-binding proteins and nucleosome position. Nat Methods 10:1213–1218.

Candia AF, Wright CV. 1995. The expression pattern of *Xenopus Mox-2* implies a role in initial mesodermal differentiation. Mech Dev. 52:27–36.

Clarke SL, et al. 2012. Human Developmental enhancers conserved between deuterostomes and protostomes. PLoS Genet. 8:e1002852.

Conesa A, et al. 2005. Blast2GO: a universal tool for annotation, visualization and analysis in functional genomics research. Bioinformatics 21:3674–3676.

Corbo JC, Levine M, Zeller RW. 1997. Characterization of a notochord-specific enhancer from the *Brachyury* promoter region of the ascidian, *Ciona intestinalis.* Development 124:589–602.

Davidson EH. 2011. Evolutionary bioscience as regulatory systems biology. Dev Biol. 357:35–40.

Dayal S, et al. 2004. Creation of *cis*-regulatory elements during sea urchin evolution by co-option and optimization of a repetitive sequence adjacent to the *spec2a* gene. Dev Biol. 273:436–453.

Dickmeis T, et al. 2001. Expression of the anti-dorsalizing morphogenetic protein gene in the zebrafish embryo. Dev Genes Evol. 211:568–572.

Dogan N, et al. 2015. Occupancy by key transcription factors is a more accurate predictor of enhancer activity than histone modifications or chromatin accessibility. Epigenetics Chromatin 8:16.

Doglio L, et al. 2013. Parallel evolution of chordate *cis*-regulatory code for development. PLoS Genet. 9:e1003904.

Fatica A, Bozzoni I. 2014. Long non-coding RNAs: new players in cell differentiation and development. Nat Rev Genet. 15:7–21.

Fidler AL, et al. 2014. A unique covalent bond in basement membrane is a primordial innovation for tissue evolution. Proc Natl Acad Sci U S A. 111:331–336.

Fisher R. 1922. On the interpretation of $\chi 2$ from contingency tables, and the calculation of P. J R Stat Soc. 85:87–94.

Frazer KA, Pachter L, Poliakov A, Rubin EM, Dubchak I. 2004. VISTA: computational tools for comparative genomics. Nucleic Acids Res. 32:W273–W279.

Furlong RF. 2005. Insights into vertebrate evolution from the chicken genome sequence. Genome Biol. 6:207.

Gardner PP, et al. 2011. Rfam: Wikipedia, clans and the "decimal" release. Nucleic Acids Res. 39:D141–D145.

Grabherr MG, et al. 2011. Full-length transcriptome assembly from RNA-Seq data without a reference genome. Nat Biotechnol. 29:644–652.

Guil S, Esteller M. 2012. *Cis*-acting noncoding RNAs: friends and foes. Nat Struct Mol Biol. 19:1068–1075.

Harris RS. 2007. Improved pairwise alignment of genomic DNA. Ph.D. dissertation, Pennsylvania State University.

Hausser J, Zavolan M. 2014. Identification and consequences of miRNA-target interactions - beyond repression of gene expression. Nat Rev Genet. 15:599–612.

Heinz S, et al. 2010. Simple combinations of lineage-determining transcription factors prime *cis*-regulatory elements required for macrophage and B cell identities. Mol Cell. 38:576–589.

Hemberg M, et al. 2012. Integrated genome analysis suggests that most conserved non-coding sequences are regulatory factor binding sites. Nucleic Acids Res. 40:7858–7869.

Hiller M, Schaar BT, Bejerano G. 2012. Hundreds of conserved non-coding genomic regions are independently lost in mammals. Nucleic Acids Res. 40:11463–11476.

Holland LZ, et al. 2008. The amphioxus genome illuminates vertebrate origins and cephalochordate biology. Genome Res. 18:1100–1111.

Holland LZ, Yu JK. 2004. Cephalochordate (amphioxus) embryos: procurement, culture, and basic methods. Methods Cell Biol. 74:195–215.

Holland ND, Holland LZ, Heimberg A. 2015. Hybrids between the Florida amphioxus (*Branchiostoma floridae*) and the Bahamas lancelet (*Asymmetron lucayanum*): developmental morphology and chromosome counts. Biol Bull. 228:13–24.

Holland PW, Koschorz B, Holland LZ, Herrmann BG. 1995. Conservation of *Brachyury (T)* genes in amphioxus and vertebrates: developmental and evolutionary implications. Development 121:4283–4291.

Huang S, et al. 2014. Decelerated genome evolution in modern vertebrates revealed by analysis of multiple lancelet genomes. Nat Commun. 5:5896.

Hufton AL, et al. 2009. Deeply conserved chordate noncoding sequences preserve genome synteny but do not drive gene duplicate retention. Genome Res. 19:2036–2051.

Irimia M, et al. 2012a. Comparative genomics of the *Hedgehog* loci in chordates and the origins of *Shh* regulatory novelties. Sci Rep. 2:433.

Irimia M, et al. 2012b. Extensive conservation of ancient microsynteny across metazoans due to *cis*-regulatory constraints. Genome Res. 22:2356–2367.

Irvine SQ. 2013. Study of *cis*-regulatory elements in the ascidian *Ciona intestinalis.* Curr Genomics. 14:56–67.

Ishibashi M, Noda AO, Sakate R, Imanishi T. 2012. Evolutionary growth process of highly conserved sequences in vertebrate genomes. Gene 504:1–5.

Jagla T, et al. 1999. Plasticity within the lateral somatic mesoderm of *Drosophila* embryos. Int J Dev Biol. 43:571–573.

Kajitani R, et al. 2014. Efficient de novo assembly of highly heterozygous genomes from whole-genome shotgun short reads. Genome Res. 24:1384–1395.

Katoh K, Standley DM. 2013. MAFFT multiple sequence alignment software version 7: improvements in performance and usability. Mol Biol Evol. 30:772–780.

Kawakami K, et al. 2004. A transposon-mediated gene trap approach identifies developmentally regulated genes in zebrafish. Dev Cell 7:133–144.

Kon T, et al. 2007. Phylogenetic position of a whale-fall lancelet (Cephalochordata) inferred from whole mitochondrial genome sequences. BMC Evol Biol. 7:127.
Kozomara A, Griffiths-Jones S. 2013. miRBase: annotating high confidence microRNAs using deep sequencing data. Nucleic Acids Res. 42:D68–D73.
Lang M, et al. 2010. Conservation of *shh cis*-regulatory architecture of the coelacanth is consistent with its ancestral phylogenetic position. Evodevo 1:11.
Li H, et al. 2009. The Sequence Alignment/Map format and SAMtools. Bioinformatics 25:2078–2079.
Lunter G, Goodson M. 2011. Stampy: a statistical algorithm for sensitive and fast mapping of Illumina sequence reads. Genome Res. 21:936–939.
Maeso I, Irimia M, Tena JJ, Casares F, Gómez-Skarmeta JL. 2013. Deep conservation of *cis*-regulatory elements in metazoans. Philos Trans R Soc Lond B Biol Sci. 368:20130020.
Maeso I, et al. 2012. An ancient genomic regulatory block conserved across bilaterians and its dismantling in tetrapods by retrogene replacement. Genome Res. 22:642–655.
Maeso I, Tena JJ. 2016. Favorable genomic environments for *cis*-regulatory evolution: a novel theoretical framework. Semin Cell Dev Biol. 57:2–10.
Makunin IV, Kolesnikova TD, Andreyenkova NG. 2014. Underreplicated regions in *D. melanogaster* are enriched with fast evolving genes and highly conserved noncoding sequences. Genome Biol Evol. 6:2050–2060.
Manzanares M, et al. 2000. Conservation and elaboration of *Hox* gene regulation during evolution of the vertebrate head. Nature 408:854–857.
Marçais G, Kingsford C. 2011. A fast, lock-free approach for efficient parallel counting of occurrences of *k*-mers. Bioinformatics 27:764–770.
Martinez-Morales JR. 2015. Toward understanding the evolution of vertebrate gene regulatory networks: comparative genomics and epigenomic approaches. Brief Funct Genomics 15(4):315–321.
McEwen GK, et al. 2009. Early evolution of conserved regulatory sequences associated with development in vertebrates. PLoS Genet. 5:e1000762.
McKenna A, et al. 2010. The genome analysis toolkit: a MapReduce framework for analyzing next-generation DNA sequencing data. Genome Res. 20:1297–1303.
Meader S, Ponting CP, Lunter G. 2010. Massive turnover of functional sequence in human and other mammalian genomes. Genome Res. 20:1335–1343.
Minguillón C, Garcia-Fernàndez J. 2002. The single amphioxus *Mox* gene: insights into the functional evolution of *Mox* genes, somites, and the asymmetry of amphioxus somitogenesis. Dev. Biol. 246:455–465.
Nawrocki EP, Kolbe DL, Eddy SR. 2009. Infernal 1.0: inference of RNA alignments. Bioinformatics 25:1335–1337.
Nelson AC, Wardle FC. 2013. Conserved non-coding elements and *cis* regulation: actions speak louder than words. Development 140:1385–1395.
Nguyen PD, et al. 2014. Haematopoietic stem cell induction by somite-derived endothelial cells controlled by *meox1*. Nature 512:314–318.
Nohara M, Nishida M, Miya M, Nishikawa T. 2005. Evolution of the mitochondrial genome in cephalochordata as inferred from complete nucleotide sequences from two epigonichthys species. J Mol Evol. 60:526–537.
Ono H, Kozmik Z, Yu JK, Wada H. 2014. A novel N-terminal motif is responsible for the evolution of neural crest-specific gene-regulatory activity in vertebrate *FoxD3*. Dev Biol. 385:396–404.
Van Otterloo E, et al. 2012. Novel *Tfap2*-mediated control of *soxE* expression facilitated the evolutionary emergence of the neural crest. Development 139:720–730.
Parker HJ, Sauka-Spengler T, Bronner M, Elgar G. 2014. A reporter assay in lamprey embryos reveals both functional conservation and elaboration of vertebrate enhancers. PLoS One 9:e85492.
Pascual-Anaya J, D'Aniello S, Garcia-Fernàndez J. 2008. Unexpectedly large number of conserved noncoding regions within the ancestral chordate *Hox* cluster. Dev Genes Evol. 218:591–597.
Patel RK, Jain M. 2012. NGS QC toolkit: a toolkit for quality control of next generation sequencing data. PLoS One 7:e30619.
Paten B, et al. 2011. Cactus: algorithms for genome multiple sequence alignment. Genome Res. 21:1512–1528.
Pennacchio L, et al. 2006. *In vivo* enhancer analysis of human conserved non-coding sequences. Nature 444:499–502.
Putnam NH, et al. 2008. The amphioxus genome and the evolution of the chordate karyotype. Nature 453:1064–1071.
Quinlan AR, Hall IM. 2010. BEDTools: a flexible suite of utilities for comparing genomic features. Bioinformatics 26:841–842.
Ramos C, Robert B. 2005. *msh/Msx* gene family in neural development. Trends Genet. 21:624–632.
Royo JL, et al. 2011. Transphyletic conservation of developmental regulatory state in animal evolution. Proc Natl Acad Sci U S A. 108:14186–14191.
Russo MT, et al. 2004. Regulatory elements controlling *Ci-msxb* tissue-specific expression during *Ciona intestinalis* embryonic development. Dev Biol. 267:517–528.
Sanges R, et al. 2013. Highly conserved elements discovered in vertebrates are present in non-syntenic loci of tunicates, act as enhancers and can be transcribed during development. Nucleic Acids Res. 41:3600–3618.
Saudemont A, et al. 2008. Complementary striped expression patterns of *NK* homeobox genes during segment formation in the annelid Platynereis. Dev Biol. 317:430–443.
Schmid KJ, Tautz D. 1997. A screen for fast evolving genes from *Drosophila*. Proc Natl Acad Sci U S A. 94:9746–9750.
Schmieder R, Edwards R. 2011a. Fast identification and removal of sequence contamination from genomic and metagenomic datasets. PLoS One 6:e17288.
Schmieder R, Edwards R. 2011b. Quality control and preprocessing of metagenomic datasets. Bioinformatics 27:863–864.
Schulte-Merker S, van Eeden FJ, Halpern ME, Kimmel CB, Nüsslein-Volhard C. 1994. *no tail (ntl)* is the zebrafish homologue of the mouse *T (Brachyury)* gene. Development 120:1009–1015.
Sharman AC, Shimeld SM, Holland PWH. 1999. An amphioxus *Msx* gene expressed predominantly in the dorsal neural tube. Dev Genes Evol. 209:260–263.
Simakov O, et al. 2015. Hemichordate genomes and deuterostome origins. Nature 527:459–465.
Slater GSC, Birney E. 2005. Automated generation of heuristics for biological sequence comparison. BMC Bioinformatics 6:31.
Stanke M, Steinkamp R, Waack S, Morgenstern B. 2004. AUGUSTUS: a web server for gene finding in eukaryotes. Nucleic Acids Res. 32:W309–W312.
Stergachis AB, et al. 2014. Conservation of trans-acting circuitry during mammalian regulatory evolution. Nature 515:365–370.
The ENCODE Project Consortium 2007. Identification and analysis of functional elements in 1% of the human genome by the ENCODE pilot project. Nature 447:799–816.
Tsagkogeorga G, Turon X, Galtier N, Douzery EJP, Delsuc F. 2010. Accelerated evolutionary rate of housekeeping genes in tunicates. J Mol Evol. 71:153–167.
Valouev A, et al. 2008. Genome-wide analysis of transcription factor binding sites based on ChIP-Seq data. Nat Methods 5:829–834.
Vavouri T, McEwen GK, Woolfe A, Gilks WR, Elgar G. 2006. Defining a genomic radius for long-range enhancer action: duplicated conserved non-coding elements hold the key. Trends Genet. 22:5–10.

Vavouri T, Walter K, Gilks WR, Lehner B, Elgar G. 2007. Parallel evolution of conserved non-coding elements that target a common set of developmental regulatory genes from worms to humans. Genome Biol. 8:R15.

Venkatesh B, et al. 2014. Elephant shark genome provides unique insights into gnathostome evolution. Nature 505:174–179.

Villar D, et al. 2015. Enhancer evolution across 20 mammalian species. Cell 160:554–566.

Wada H, Escriva H, Zhang S, Laudet V. 2006. Conserved RARE localization in amphioxus *Hox* clusters and implications for *Hox* code evolution in the vertebrate neural crest. Dev Dyn. 235:1522–1531.

Waterhouse AM, Procter JB, Martin DMA, Clamp M, Barton GJ. 2009. Jalview Version 2-A multiple sequence alignment editor and analysis workbench. Bioinformatics 25:1189–1191.

Woolfe A, et al. 2005. Highly conserved non-coding sequences are associated with vertebrate development. PLoS Biol. 3:e7.

Yousaf A, Sohail Raza M, Ali Abbasi A. 2015. The evolution of bony vertebrate enhancers at odds with their coding sequence landscape. Genome Biol Evol. 7:2333–2343.

Yu JK, Holland ND, Holland LZ. 2004. Tissue-specific expression of *FoxD* reporter constructs in amphioxus embryos. Dev Biol. 274:452–461.

Yue JX, Yu JK, Putnam NH, Holland LZ. 2014. The transcriptome of an amphioxus, *Asymmetron lucayanum*, from the Bahamas: a window into chordate evolution. Genome Biol Evol. 6:2681–2696.

Associate editor: B. Venkatesh